Mid-depth recirculation observed in the interior Labrador and Irminger seas by direct velocity measurements

Kara L. Lavender*, Russ E. Davis* & W. Brechner Owens†

** Scripps Institution of Oceanography, University of California, San Diego, La Jolla, California 92093-0230, USA*
† Woods Hole Oceanographic Institution, Woods Hole, Massachusetts 02543, USA

The Labrador Sea is one of the sites where convection exports surface water to the deep ocean in winter as part of the thermohaline circulation. Labrador Sea water is characteristically cold and fresh, and it can be traced at intermediate depths (500–2,000 m) across the North Atlantic Ocean, to the south and to the east of the Labrador Sea[1–3]. Widespread observations of the ocean currents that lead to this distribution of Labrador Sea water have, however, been difficult and therefore scarce. We have used more than 200 subsurface floats to measure directly basin-wide horizontal velocities at various depths in the Labrador and Irminger seas. We observe unanticipated recirculations of the mid-depth (~700 m) cyclonic boundary currents in both basins, leading to an anticyclonic flow in the interior of the Labrador basin. About 40% of the floats from the region of deep convection left the basin within one year and were rapidly transported in the anticyclonic flow to the Irminger basin, and also eastwards into the subpolar gyre. Surprisingly, the float tracks did not clearly depict the deep western boundary current, which is the expected main pathway of Labrador Sea water in the thermohaline circulation. Rather, the flow along the boundary near Flemish Cap is dominated by eddies that transport water offshore. Our detailed observations of the velocity structure with a high data coverage suggest that we may have to revise our picture of the formation and spreading of Labrador Sea water, and future studies with similar instrumentation will allow new insights on the intermediate depth ocean circulation.

In the North Atlantic, surface waters of the meridional overturning circulation transport heat to high latitudes, where deep convection forms intermediate and deep waters in localized regions.

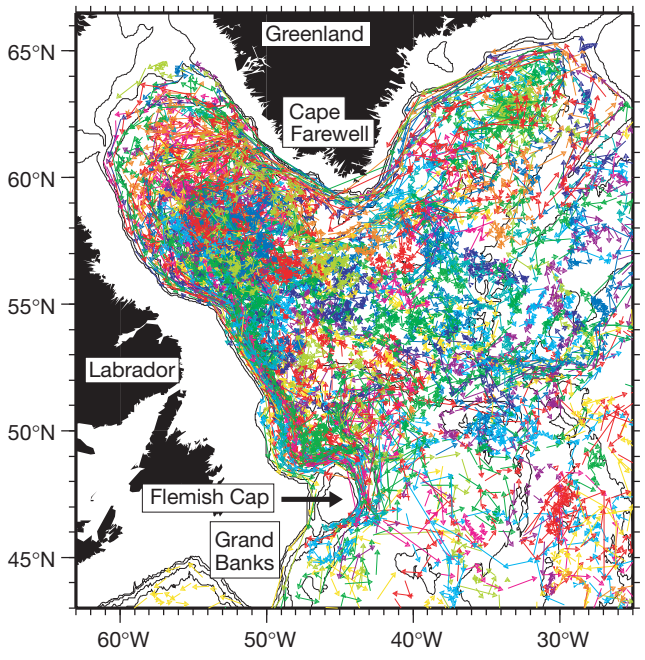

Figure 1 Trajectories of floats in the Labrador and Irminger seas at nominal depths of 400, 700 and 1,500 m. Each float is represented by one colour, and each arrow represents one subsurface drift cycle. Gaps between arrows represent the time the float was at the surface. Data shown are from November 1994 to the end of April 1999, representing over 200 years of data. Contours mark the 500-m, 1,000-m, 2,000-m, 3,000-m and 4,000-m isobaths.

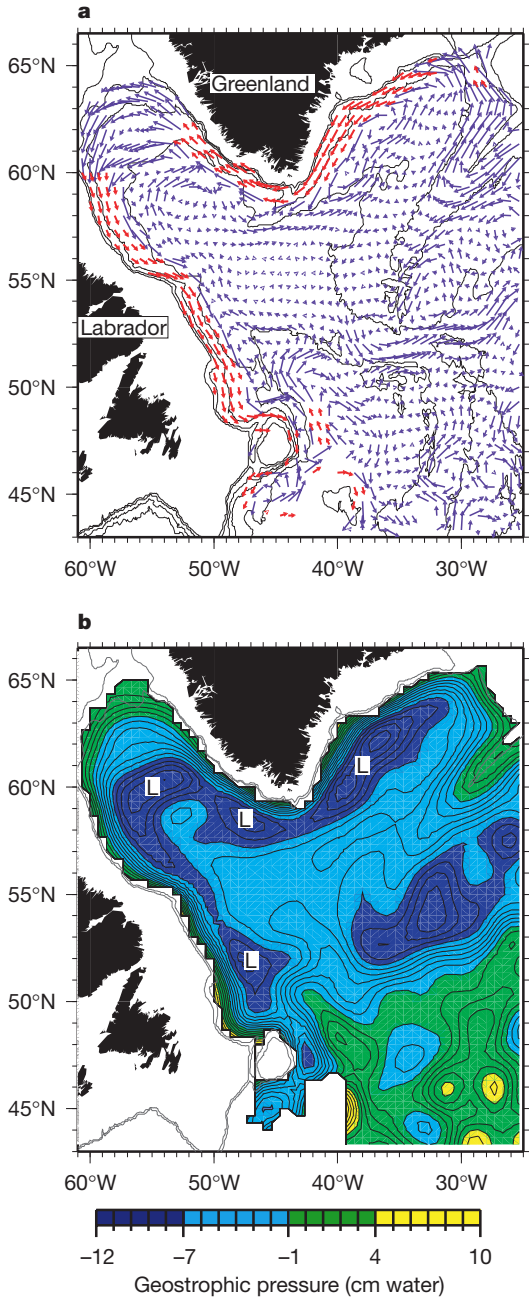

Figure 2 Objectively mapped mean circulation at 700 m depth. **a**, Velocity shown as displacement vectors. Blue arrows indicate distance travelled over 30 days for speeds $< 5\ \mathrm{cm\ s^{-1}}$; red arrows indicate distance travelled over 8 days for speeds $\geq 5\ \mathrm{cm\ s^{-1}}$. Contours mark isobaths as in Fig. 1. **b**, Geostrophic pressure measured in centimetres of water (black contours). 'L's mark selected low-pressure centres, and grey contours mark the 500-m and 1,000-m isobaths. To construct these maps, velocity data from all drift depths were corrected to 700 m using geostrophic shears from the Levitus climatology[20,21], and were averaged in bins roughly 100 km square. These data were then objectively mapped using a gaussian covariance function with a decorrelation length scale of 185 km and noise derived from the variance of the velocity field.

© 2000 Macmillan Magazines Ltd

Long-term variability in the formation process[4,5], and subsequent spreading of these water masses, may alter the meridional heat flux, a central component of the climate system[6]. Labrador Sea water (LSW), located between depths of 500 and 2,000 m, is formed in winter in the interior of the basin where cold, dry, offshore winds force convective overturning. Although hydrographic data have identified locations of deep convection[7] and have inferred a cyclonic general circulation in the Labrador Sea[8], direct velocity measurements have been limited to point measurements from a few moored current meters[9,10]. Consequently the residence time and pathways of LSW within the basin, and its exit routes into the North Atlantic, have mostly been inferred from indirect measurements.

As part of the World Ocean Circulation Experiment (WOCE) and the Labrador Sea Deep Convection Experiment[11], more than 200 neutrally buoyant subsurface P-ALACE floats[12] and SOLO floats[13] were deployed in the northern North Atlantic. The floats drift at nominal depths of 400 m, 700 m, or 1,500 m for preset periods between 3.5 and 20 days. At the end of its cycle time, each float ascends to the sea surface to transmit data via the Argos satellite system. The floats report position data, as well as vertical profiles of ocean temperature and salinity measured upon ascent or descent.

Since November 1994, more than 7,400 profiles of temperature and salinity and more than 200 years (cumulative) of drift-velocity data have been collected (Fig. 1). The drift-velocity data were used to objectively map the mean circulation at 700 m depth (Fig. 2). The strongest flows in the mean field are along the coasts of Greenland (East and West Greenland currents) and Labrador (Labrador Current), with speeds reaching 12 cm s^{-1}. The North Atlantic Current meanders eastwards at 3–7 cm s^{-1} from northeast of Flemish Cap, the topographic feature centred at 47.5° N, 45° W. The most notable feature is the unexpected anticyclonic countercurrent to the interior of the boundary currents. This anticyclonic flow is comprised of a series of recirculations that are visible as closed regions of cyclonic flow in Fig. 2a, and as low-pressure centres marked with an 'L' in Fig. 2b. This flow has not been described in circulation regimes inferred from hydrography[8,9], although northward flow to the interior of the Labrador Current was measured with current meters at one location[7].

The circulation patterns described above appear at all three drift depths and at all times of year. The flow in the upper 1,000 m is generally faster than that below, particularly in the boundary currents and in the anticyclonic flow northeast of Flemish Cap, where speeds weaken at depth by up to 5.5 cm s^{-1}. Although seasonal variability in the boundary currents could not be resolved, the recirculation to the north of Flemish Cap is faster in winter (January–April) than in summer (July–October), whereas the reverse is true of the recirculation in the western Irminger basin. The Flemish Cap recirculation appears to be fed by the Labrador Current, whose seasonal variability has been linked to variations in wind forcing[10].

Mixed-layer depths computed from temperature profiles for the winters of 1997 and 1998 (Fig. 3) show that convectively mixed layers deeper than 400 m were scattered across the basin interior, but the deepest mixed layers ($>$ 800 m) were concentrated in the western basin. This augments the picture found from a hydrographic survey[11] in February–March 1997. The floats also measured recently formed deep mixed layers as late as mid-April, and in regions outside the western basin. Mixed layers in 1998 were shallower than in 1997, indicative of the interannual variability in LSW formation[5].

Changes in heat content between consecutive vertical profiles of temperature provide a measure of the air–sea heat flux. The greatest computed average winter heat flux (-345 ± 95 W m^{-2}) occurred in the northern third of the basin, whereas the central portion containing the deepest mixed layers had an average winter heat flux of only -49 ± 46 W m^{-2}. Therefore the circulation within the western basin must be an important factor in determining where deep convection occurs.

Previous work[7] suggests that a winter cyclonic gyre in the western Labrador basin traps surface waters in a region that is repeatedly exposed to cold offshore winds. The resulting heat loss to the atmosphere then sustains deep convection. To investigate the existence of a localized gyre, the mean velocity field was mapped

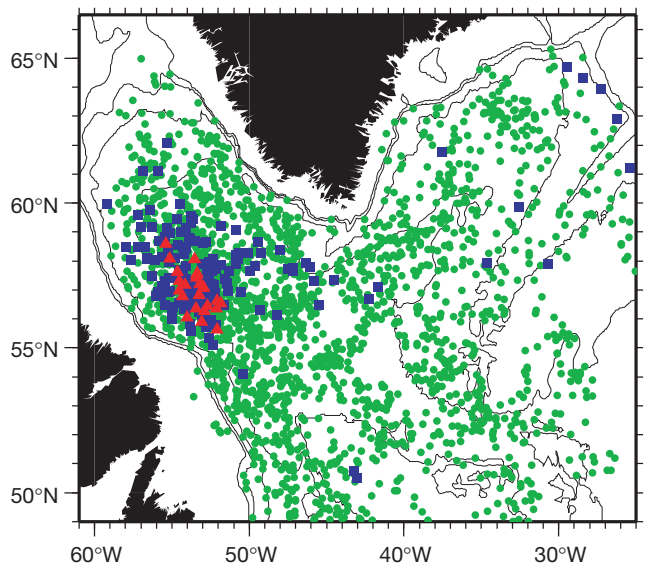

Figure 3 Winter mixed-layer depth for profiles measured in winters 1996–97 and 1997–98. The mixed-layer depth (MLD) is defined by the break between a least-squares fit of a straight line to the upper layer, and a second-order polynomial plus exponential fit to the lower layer, of each temperature profile. MLD $\leq$ 400 m are marked with green circles, 400 $<$ MLD $\leq$ 800 m with blue squares, and MLD $>$ 800 m with red triangles. Contours mark isobaths as in Fig. 1. The deepest mixed layers are located in the western basin, although mixed layers deeper than 400 m are found outside this region as well.

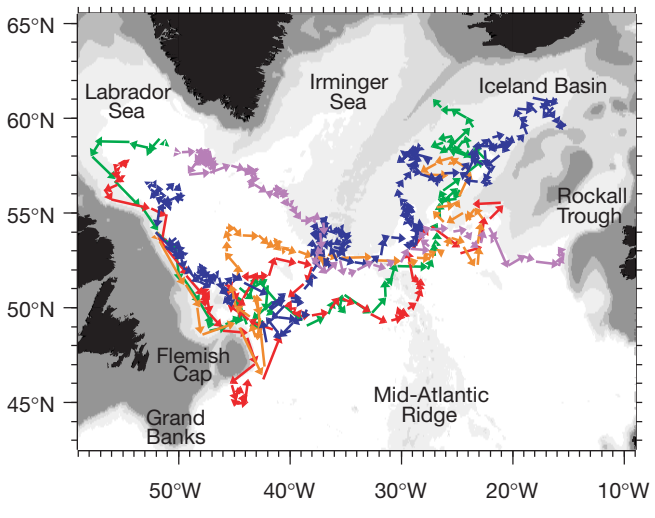

Figure 4 Trajectories of five floats that travelled from the central Labrador Sea to the eastern North Atlantic. Red, orange and green arrows indicate three floats drifting at 700 m depth; blue and purple arrows indicate two floats drifting at a depth of 1,500 m. From light to dark grey, shading indicates bathymetry $<$ 3,000 m, $<$ 2,000 m, $<$ 1,000 m and $<$ 500 m. One float (purple) left the Labrador Sea in the unexpected anticyclonic current south of Greenland and arrived at Rockall trough after only 2.8 years. The other four floats drifted in an eastward flow fed by the Labrador Current, with travel times comparable to previous estimates of spreading rates.

© 2000 Macmillan Magazines Ltd

from winter data only (not shown). Nearly all of the deepest mixed layers were located within a weak (1.8 cm s^{-1}) cyclonic recirculation, centred near 56.5° N between the Labrador Current and the interior flow. This gyre is, however, masked by variability, suggesting that the important factor is the generally weak flow in the region. Floats that recorded the deepest convection remained in the region an average of 34.5 days, and in some cases up to 110 days, before measuring the deep mixed layers. There may be a localized winter cyclonic gyre in the convection region, but (more importantly) the sluggish flow retains water there for an extended period of time, during which the water experiences a large net heat loss that drives progressively deeper convection.

From the formation region, two main routes exist for LSW to leave the Labrador Sea. The first is an eastward outflow between 51° N and 54° N, fed by the Labrador Current. Three floats drifting at 700 m and one float drifting at 1,500 m followed this path to the eastern North Atlantic (Fig. 4). The floats' travel times compare well with spreading estimates inferred from tracers[3]. Floats at 700 m depth reached the Iceland basin in 1.6–2.6 years, at an average subsurface speed (including small-scale features) of 8.7 cm s^{-1}, while the 1,500-m-deep float arrived in 3.8 years, at an average subsurface speed of 6.6 cm s^{-1}.

The second pathway out of the Labrador Sea is in the anticyclonic countercurrent flowing from the interior of the basin into the Irminger Sea. Evidence that LSW travels directly to the Irminger basin is given by high concentrations of chlorofluorocarbons (CFCs) at intermediate depths[3,14], indicative of recently ventilated water. One 1,500-m-deep float (purple in Fig. 4) left the Labrador Sea in this countercurrent, and reached the eastern edge of the North Atlantic basin at Rockall trough in 2.8 years (average speed of 4.9 cm s^{-1}). The travel time via this alternative route across the basin is 1–1.5 years faster than previous estimates from tracers[3].

LSW properties have also been traced south along the western boundary into the subtropical gyre[1,15], presumably having travelled in the deep western boundary current (DWBC). Surprisingly, none of the 1,500-m floats sampled the DWBC south of Flemish Cap (Fig. 5). The flow near Flemish Cap is strongly baroclinic, with the southward DWBC located inshore of the 4,000-m isobath[15] and below the northward, surface-intensified North Atlantic Current (NAC). At the surface, some floats were carried offshore by the NAC, while others drifted onshore towards the DWBC region. At depth, a number of floats sampled an expected southward flow inshore of the 3,000-m isobath north of ~47° N, with average measured speeds of up to 24.7 cm s^{-1}. Near Flemish Cap, however, a number of floats underwent cross-isobath flow with comparable speeds. The flow at the northern edge of Flemish Cap turns back to the northwest, feeding a recirculation of the interior anticyclonic countercurrent, while eastward and southeastward flow is observed throughout much of the region. The existence of these cross-isobath flows at the slope of Flemish Cap indicates a rapid exchange between the boundary current and offshore waters, and is largely responsible for the lack of floats travelling southward into the subtropical gyre. Measurements[16] of high eddy kinetic energy east of Flemish Cap suggest that these flows are eddy-driven.

Floats that travelled along the western boundary and recirculated to the northwest near Flemish Cap did not measure significant variations in temperature and salinity at depths of 1,000–1,500 m, indicating this is a pathway of LSW. Most floats travelling east of ~42° W, however, encountered the warmer and saltier water of the NAC at these depths. Hydrographic data[17] show a deepening of isopycnals to the east of Flemish Cap, suggesting that LSW is still present in this region but below the depth of the floats (1,500 m). Thus both deep pathways described above transport LSW away from the western boundary.

Although floats did not drift south along the western boundary beyond ~45° N, tracer studies[1,17] clearly indicate that LSW does reach the subtropical gyre, presumably in the DWBC. One reason that the floats did not measure the boundary current may be high variability in the flow field near Flemish Cap, which might make intermittent the southward flow of LSW in the DWBC[17]. Another possibility is that LSW reaches the subtropical gyre further east, in recirculations on either side of the Mid-Atlantic Ridge[18,19]. The questions of how and when intermediate and deep waters enter the subtropical gyre, and whether or not this exchange could be shut off by climate variability, are essential to understanding the long-term behaviour of the thermohaline circulation. These questions cannot be answered with the present observations. □

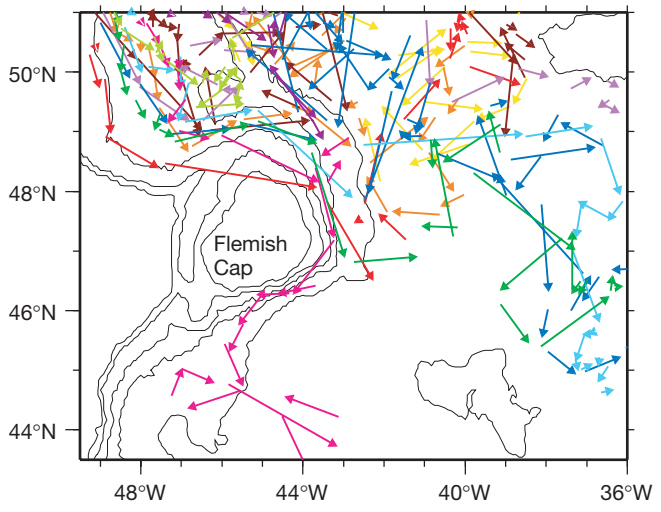

Figure 5 Displacements of floats drifting at 1,500 m depth near Flemish Cap. Colour scheme and bathymetric contours as in Fig. 1. There is no indication of a coherent southward flow along the boundary south of Flemish Cap. Instead deep, cross-isobath flows are observed, which provide a rapid exchange between the boundary and offshore waters.

Received 2 March; accepted 22 June 2000.

1. Talley, L. D. & McCartney, M. S. Distribution and circulation of Labrador Sea Water. *J. Phys. Oceanogr.* **12,** 1189–1205 (1982).
2. Cunningham, S. A. & Haine, T. W. N. Labrador Sea Water in the Eastern North Atlantic. Part I: A synoptic circulation inferred from a minimum in potential vorticity. *J. Phys. Oceanogr.* **25,** 649–665 (1995).
3. Sy, A. *et al.* Surprisingly rapid spreading of newly formed intermediate waters across the North Atlantic Ocean. *Nature* **386,** 675–679 (1997).
4. Dickson, R. From the Labrador Sea to global change. *Nature* **386,** 649–650 (1997).
5. Dickson, R., Lazier, J., Meincke, J., Rhines, P. & Swift, J. Long-term coordinated changes in the convective activity of the North Atlantic. *Prog. Oceanogr.* **38,** 241–295 (1996).
6. Bryden, H. L. in *Interactions Between Global Climate Subsystems, The Legacy of Hann* (eds McBean, G. A. & Hantel, M.) 65–75 (American Geophysical Union, Washington DC, 1993).
7. Clarke, R. A. & Gascard, J.-C. The formation of Labrador Sea Water. I. Large-scale processes. *J. Phys. Oceanogr.* **13,** 1764–1778 (1983).
8. Lazier, J. R. N. The renewal of Labrador Sea Water. *Deep-Sea Res.* **20,** 341–353 (1973).
9. Clarke, R. A. Transport through the Cape Farewell–Flemish Cap section. *Rapp. P.-v. Réun. Cons. Int. Explor. Mer.* **185,** 120–130 (1984).
10. Lazier, J. R. N. & Wright, D. G. Annual velocity variations in the Labrador Current. *J. Phys. Oceanogr.* **23,** 659–678 (1993).
11. Lab Sea Group. The Labrador Sea Deep Convection Experiment. *Bull. Am. Meteorol. Soc.* **79,** 2033–2058 (1998).
12. Davis, R. E., Webb, D. C., Regier, L. A. & Dufour, J. The autonomous Lagrangian circulation explorer (ALACE). *J. Atmos. Ocean. Technol.* **9,** 264–285 (1992).
13. Davis, R. E., Sherman, J. T. & Dufour, J. Profiling ALACEs and other advances in autonomous subsurface floats. *J. Atmos. Oceanic Technol.* (submitted).
14. Min, D. H. *Studies of Large-scale Intermediate and Deep Water Circulation and Ventilation in the North Atlantic, South Indian and Northeast Pacific Oceans, and in the East Sea (Sea of Japan), using Chlorofluorocarbons as Tracers.* Thesis, Univ. California, San Diego (1999).
15. Pickart, R. S., Smethie, W. M., Lazier, J. R. N., Jones, E. P. & Jenkins, W. J. Eddies of newly formed upper Labrador Sea Water. *J. Geophys. Res.* **101,** 20711–20726 (1996).
16. Carr, M.-E. & Rossby, T. Pathways of transport in the North Atlantic Current from surface drifters and subsurface floats. *J. Geophys. Res.* (submitted).
17. Pickart, R. S., Spall, M. A. & Lazier, J. R. N. Mid-depth ventilation in the western boundary current system of the sub-polar gyre. *Deep-Sea Res.* **44,** 1025–1054 (1997).
18. Lozier, M. S. Evidence for large-scale eddy-driven gyres in the North Atlantic. *Science* **277,** 361–364 (1997).

© 2000 Macmillan Magazines Ltd

19. Paillet, J., Arhan, M. & McCartney, M. S. Spreading of Labrador Sea Water in the eastern North Atlantic. *J. Geophys. Res.* **103,** 10223–10239 (1998).
20. Levitus, S., Burgett, R. & Boyer, T. P. *World Ocean Atlas 1994* Vol. 3, *Salinity* (NOAA Atlas NESDIS 3, US Department of Commerce, Washington, DC, 1994).
21. Levitus, S. & Boyer, T. P. *World Ocean Atlas 1994* Vol. 4, *Temperature* (NOAA Atlas NESDIS 4, US Department of Commerce, Washington DC, 1994).

Acknowledgements

We thank J. Dufour, J. Sherman, J. Valdes, R. Tavares and B. Guest for technical development and preparation of the floats, D. Newton and C. Wooding for help with data processing, and the numerous scientists who deployed the floats, often in adverse conditions at sea. This work was supported by the National Science Foundation, the Office of Naval Research, and the National Oceanic and Atmospheric Administration.

Correspondence and requests for materials should be addressed to K.L.L. (e-mail: klavender@ucsd.edu)

Earthquakes as beacons of stress change

Leonardo Seeber & John G. Armbruster

Lamont-Doherty Earth Observatory, Palisades, New York 10964, USA

Aftershocks occurring on faults in the far-field of a large earthquake rupture can generally be accounted for by changes in static stress on these faults caused by the rupture[1,2]. This implies that faults interact, and that the timing of an earthquake can be affected by previous nearby ruptures[3–6]. Here we explore the potential of small earthquakes to act as 'beacons' for the mechanical state of the crust. We investigate the static-stress changes resulting from the 1992 Landers earthquake in southern California which occurred in an area of high seismic activity stemming from many faults. We first gauge the response of the regional seismicity to the Landers event with a new technique, and then apply the same method to the inverse problem of determining the slip distribution on the main rupture from the seismicity. Assuming justifiable parameters, we derive credible matches to slip profiles obtained directly from the Landers mainshock[7,8]. Our results provide a way to monitor mechanical conditions in the upper crust, and to investigate processes leading to fault failure.

The mechanical state of a fault can be characterized by Coulomb stress[9] $CS = \tau - \mu(\sigma_n - p)$, a scalar, where τ is shear stress, σ_n is normal stress, μ is the coefficient of friction, and p is the pore pressure. In general, CS is not known, but a "beacon" fault will experience a static stress change $\Delta CS = \Delta\tau - \mu'\Delta\sigma_n$ from a known shear dislocation on a causative fault[10] (the "rupture"). In a linear isotropic elastic medium ΔCS is a scalar. In this simple formulation, the effective friction parameter μ' includes a possible change in pore pressure, but is independent of space and time. $\Delta CS \ll CS$ for beacons sufficiently far from the rupture (7.5 km in this case; Fig. 1) and only the component of $\Delta\tau$ parallel to the beacon's slip vector is consequential. $\Delta CS > 0$ is expected to 'encourage' the beacon fault toward failure; $\Delta CS < 0$ is expected to 'discourage' it from failing. This expectation can be tested for earthquakes that are resolved as shear failures with specific location, strike, dip and rake. In general, ΔCS is significant within a rupture-length of any rupture[11]. Both deformation and stress changes, however, are dominated by the largest ruptures[12]. We consider the classical interaction experiment where ΔCS stems from a large rupture and affects a multitude of beacon earthquakes that are assumed to be too small to mutually interact[1].

The 1992 Landers sequence in southern California provides the causative rupture in this experiment: it is dominated by the 28 June, $M_W = 7.2$ mainshock and includes the 23 April, $M_L = 6.1$ Joshua Tree 'foreshock' and the 28 June, $M_L = 6.5$ Big Bear 'aftershock' (Fig. 1). The rupture is within a broad zone of seismicity associated with the plate boundary. A set of relocated and quality-selected focal mechanisms for most $M \geq 1.5$ earthquakes in this zone since 1980 have been interpreted for fault structure and preferred nodal planes (data are available at ftp://scec.gps.caltech.edu/pub/focal/focal1.nano). This seismicity stems from many relatively small, scattered faults ranging widely in orientation and kinematics which serve as ideal beacons for stress change[13] (Fig. 1). ΔCS is calculated for each beacon as the compound effect of 28 elemental dislocations[10] approximating the rupture[7].

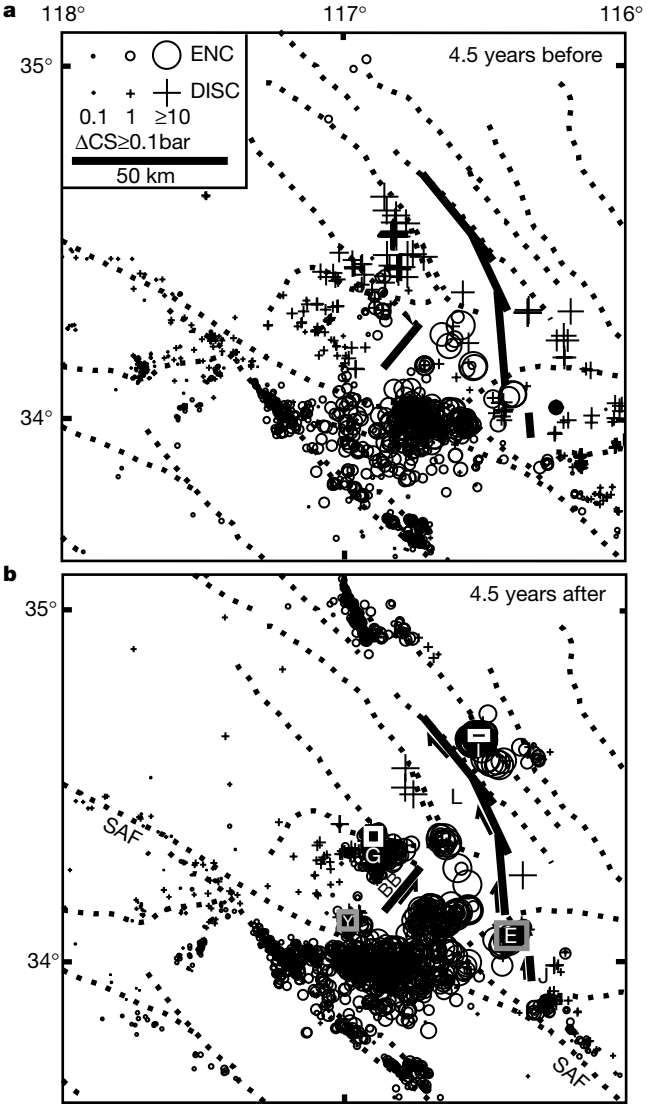

Figure 1 Earthquakes as beacons of the static stress change from the 23 April–28 June 1992 composite rupture. Heavy lines[7,9]: J, Joshua; L, Landers; BB, Big Bear. Coulomb stress change calculated for each beacon is either encouraging (ENC, $\Delta CS > 0.1$ bar; circles) or discouraging (DISC; $\Delta CS < 0.1$ bar; crosses). Beacons after the rupture (1,680 encouraged and 538 discouraged earthquakes) are expected to occur if encouraged, while beacons before the rupture (681 encouraged and 553 discouraged earthquakes) provide the reference (for example, discouraged seismicity is turned off by the rupture). Excluded are beacons less than 7.5 km from the rupture, where non-elastic interactions may occur. Friction $\mu' = 0.8$. Early discouraged earthquakes are concentrated in four clusters (boxed) where local stress interactions are suspected: G, Gold Mountain; Y, Yucaipa; E, Eureka Park; I, Iron Ridge. SAF, San Andreas fault.

© 2000 Macmillan Magazines Ltd